

2023-12-15

# Leaf thermal regulation strategies of canopy species across four vegetation types along a temperature and precipitation gradient

Zhou, Y

<https://pearl.plymouth.ac.uk/handle/10026.1/21659>

---

10.1016/j.agrformet.2023.109766

Agricultural and Forest Meteorology

Elsevier BV

---

*All content in PEARL is protected by copyright law. Author manuscripts are made available in accordance with publisher policies. Please cite only the published version using the details provided on the item record or document. In the absence of an open licence (e.g. Creative Commons), permissions for further reuse of content should be sought from the publisher or author.*

1 **Leaf thermal regulation strategies of canopy species across four vegetation types**  
2 **along a temperature and precipitation gradient**

3

4 Yingying Zhou<sup>1,2</sup>, Nawatbhris Kitudom<sup>1,2</sup>, Sophie Fauset<sup>3\*</sup>, Martijn Slot<sup>5</sup>, Zexin  
5 Fan<sup>1,4</sup>, Jianping Wang<sup>6</sup>, Weiwei Liu<sup>7</sup>, Hua Lin<sup>1,4\*</sup>

6

7 <sup>1</sup>CAS Key Laboratory of Tropical Forest Ecology, Xishuangbanna Tropical Botanical  
8 Garden, Chinese Academy of Sciences, Mengla, Yunnan 666303, China.

9 <sup>2</sup>University of Chinese Academy of Sciences, Beijing 100049, China.

10 <sup>3</sup>School of Geography, Earth and Environmental Sciences, University of Plymouth,  
11 Plymouth, PL4 8AA, UK.

12 <sup>4</sup>Ailaoshan Station for Subtropical Forest Ecosystem Studies, Xishuangbanna  
13 Tropical Botanical Garden, Chinese Academy of Sciences, Jingdong, Yunnan 676209,  
14 China.

15 <sup>5</sup>Smithsonian Tropical Research Institute, Panama City 0843-03092, Panama

16 <sup>6</sup>School of Information Engineering and Automation, Kunming University of Science  
17 and Technology, Kunming 650000, China

18 <sup>7</sup>Lijiang Forest Biodiversity National Observation and Research Station, Kunming  
19 Institute of Botany, Chinese Academy of Sciences, Lijiang, Yunnan 674100, China.

20

21

22

23

24

25

26

27

28

29

30

31

32 **Abstract**

33       The ecophysiological processes of leaves are more related to leaf temperature  
34 (T<sub>l</sub>) than air temperature (T<sub>a</sub>). Transpiration and leaf physical traits enable plants to  
35 maintain T<sub>l</sub> within a thermal range. However, it is challenging to quantitatively study  
36 leaf thermal regulation strategies, due to the complex interaction between thermal  
37 effects of transpiration and leaf physical traits. We utilized a 3-T method that  
38 compares T<sub>l</sub>, T<sub>a</sub>, and T<sub>n</sub> (the temperature of non-transpiring leaves) investigate  
39 thermal regulation strategies of dominant canopy species in four vegetation types,  
40 including a savanna woodland, a tropical rain forest, a subtropical evergreen broad-  
41 leaved forest, and a temperate mixed forest. Our results indicate that the difference  
42 between T<sub>l</sub> and T<sub>a</sub> decreased as the site mean temperature increased. Transpirational  
43 cooling was strongest in savanna woodland, and decreased from the hottest site to the  
44 coldest site. Without transpiration, sun-exposed leaves were consistently hotter under  
45 sunshine than air. This physical warming effect increased from the hottest site to the  
46 coldest site. We observed leaf area, water content and leaf angle played a significant  
47 role in physical thermal regulation. The present research quantitatively measured leaf  
48 thermal regulation strategies across a temperature and precipitation gradient, which  
49 advances our understanding of how plants adapt to their thermal environments.

50

51 **KEYWORDS:** leaf temperature, leaf traits, physical thermal effect, transpirational  
52 cooling, thermal regulation, thermal response

53

## 54 INTRODUCTION

55 Leaf temperature (T<sub>l</sub>) is the direct micro-environment governing plant  
56 ecophysiological processes (Gates, 1968; Slot and Winter, 2017), and further  
57 determines ecosystem energy, water and carbon budgets (Rey-Sánchez et al., 2017;  
58 Sánchez et al., 2009). However, leaf temperatures often deviate from air temperature  
59 (T<sub>a</sub>). Previous investigation across 62 species have revealed that in a 5°C environment,  
60 leaf temperatures can be elevated by up to 10°C compared to the surrounding air  
61 temperature. Conversely, in a 55°C environment, leaf temperatures can be  
62 approximately 7°C lower than the ambient air temperature (Michaletz et al., 2015).  
63 The temperature difference between leaf and air has also been observed to reached  
64 18.3 °C in the Atlantic forest, Brazil (Fauset et al., 2018). Similar temperature  
65 deviations from air temperature are also common in inanimate materials such as water  
66 or metal due to their distinct physical properties, for example heat capacity,  
67 reflectivity, and size. However, these properties of inanimate materials remain  
68 constant regardless of the environment. In contrast, plant traits can adapt or acclimate  
69 to various environments, enable them to maintain their leaf temperatures within a  
70 specific range. Although the time required for traits to change may vary widely,  
71 ranging from a few seconds (e.g. stomatal conductance and transpiration) to hundreds  
72 of years, plant traits are flexible. The combination of all the physical traits (e.g.,  
73 morphological traits, optical traits, material properties) and physiological leaf traits  
74 (e.g., transpiration) that contribute to maintaining leaf temperatures within the optimal  
75 temperature range for photosynthesis is referred as "thermal regulation" (Jones and

76 Rotenberg, 2011; Monteiro et al., 2016). It includes cooling effects in hot habitats and  
77 warming effects in cool habitats. Thermal regulation, thermal tolerance, and thermal  
78 avoidance together constitute thermal adaptation strategies of plants.

79 Thermal regulation capacities of leaves differ among species, and vary with the  
80 environment (Fauset *et al.*, 2018). According to the regression slope of Tl vs. Ta ( $\beta$ ),  
81 three types of leaf thermal response have been identified: limited homeothermy ( $\beta <$   
82 1), poikilothermy ( $\beta = 1$ ), and megathermy ( $\beta > 1$ ) (Blonder and Michaletz, 2018).  
83 Homeothermic leaves maintain Tl below Ta when Ta exceeds a certain threshold,  
84 while poikilothermic leaves closely track Ta (Tl = Ta), and megathermic leaves  
85 exhibit a faster increase in temperature compared to Ta. Generally, stronger thermal  
86 regulation, including both warming and cooling is found under extreme thermal  
87 environments (John-Bejai et al., 2013; Körner, 2016; Smith, 1978; Vogel, 2005),  
88 while weaker thermal regulation is found in more optimal thermal environments  
89 (Drake et al., 2020). However, the mechanisms underlying leaf thermal regulation  
90 strategies across different environmental gradients have not been fully explored.

91 Leaf temperature is determined by a combination of leaf physical and  
92 physiological traits and environmental conditions (Campbell and Norman, 1998;  
93 Monteith and Unsworth, 2013; Nobel, 2005). Leaf traits related to radiation loading  
94 and heat exchange impact leaf temperature. For example, optical traits, leaf size and  
95 orientation determine radiation loading (Jones and Rotenberg, 2011; Lambers et al.,  
96 1998), while material properties such as water content and density affect heat capacity  
97 (Jones, 2014; Lambers et al., 1998); leaf shape and area are related to heat

98 conductance ( $g_{Ha}$ ) (Leigh et al., 2012; Muller et al., 2021); Stomatal conductance ( $g_s$ )  
99 and water vapor transport conductance ( $g_{va}$ ) influence transpirational cooling (Gates,  
100 2003; Jones and Rotenberg, 2011; Monteith, 1973; Muir, 2019). However, it is  
101 challenging to study thermal effects of leaf traits in the field due to the high variability  
102 of leaf traits and their interactions (Blonder et al., 2020; Kitudom et al., 2022). For  
103 example, small leaves with dark color also have thin boundary layers, which  
104 facilitates heat exchange, meanwhile their dark colors also enables them to absorb  
105 more radiation. In reality, it is the coordination of multiple leaf traits that improves  
106 plant adaptation to the primary stress under its specific environment. Not all leaf traits  
107 contribute directly to thermal regulation. Therefore, some previous studies used  
108 artificial leaves to quantitatively evaluate thermal effects of leaf traits under controlled  
109 environments (Daudet et al., 1998; Fetcher, 1981; Vogel, 2009). Lin et al. (2017)  
110 employed a method to quantitatively distinguish thermal effects of transpiration and  
111 leaf physical traits *in situ*. This technique, called “3-T method” requires three  
112 temperatures: the temperature of a control leaf ( $T_l$ ), the temperature of a non-  
113 transpiring leaf ( $T_n$ ), and air temperature ( $T_a$ ). Although the combination of  $T_l$ ,  $T_n$   
114 and  $T_a$  has often been used to evaluate water stress, transpiration and stomatal  
115 conductance (Jones, 1999; Jones et al., 2018; Jones and Rotenberg, 2011; Qiu et al.,  
116 2002), Lin et al. (2017) firstly used it to quantify thermal regulation in the field. By  
117 employing this method, researchers can effectively monitor the thermal effects of  
118 transpiration and the physical traits of leaves separately, thereby revealing leaf  
119 thermal regulation strategies and their response to the natural environment *in situ*.

120 Upper-canopy species are fully exposed to air and solar radiation. Compared  
121 with shaded plants, they are more influenced by radiative heating, turbulent exchange,  
122 and longwave radiation loss at night (Miller et al., 2021). Transient “lulls” in wind can  
123 cause leaf temperature to rise by  $> 5$  °C in just a few seconds (Vogel, 2005). The  
124 highly exposed and fluctuating environment makes canopy leaves more susceptible to  
125 temperature extremes. Maximum temperatures of upper-canopy leaves have been  
126 shown to exceed photosynthetic thermal optima in several tropical forests (Doughty  
127 and Goulden, 2008; Mau et al., 2018; Miller et al., 2021; Pau et al., 2018). In such a  
128 fluctuating environment, traits associated with temperature regulation should incur  
129 greater selective advantage than in understory conditions. In addition, understory  
130 species are distributed in buffered micro-environments due to shading which might be  
131 very different from the canopy environment (Vinod et al., 2023). Therefore, canopy  
132 species more strongly reflect the interaction between plants and the local environment  
133 (Still et al., 2021).

134 In the present research, we used the 3-T method to study thermal regulation  
135 strategies of upper canopy species in a savanna woodland, a tropical rain forest, a  
136 subtropical evergreen broad-leaved forest and a temperate mixed forest. Thermal  
137 regulation strategies depend on the temperature and water status of the habitat (Fauset  
138 et al., 2018; Gates, 2003; Jones and Rotenberg, 2011). We hypothesize that the  
139 savanna species mainly depend on leaf physical traits to cool leaves due to limited  
140 transpirational cooling under dry conditions; tropical rain forest species can utilize  
141 both transpirational cooling and leaf physical traits to avoid high leaf temperatures;

142 while subtropical forest species exhibit weaker thermal regulation due to limited  
143 thermal stress; the species in the temperate forest primarily rely on physical warming  
144 to cope with cold stress.

## 145 MATERIALS AND METHODS

### 146 Study sites and plant species

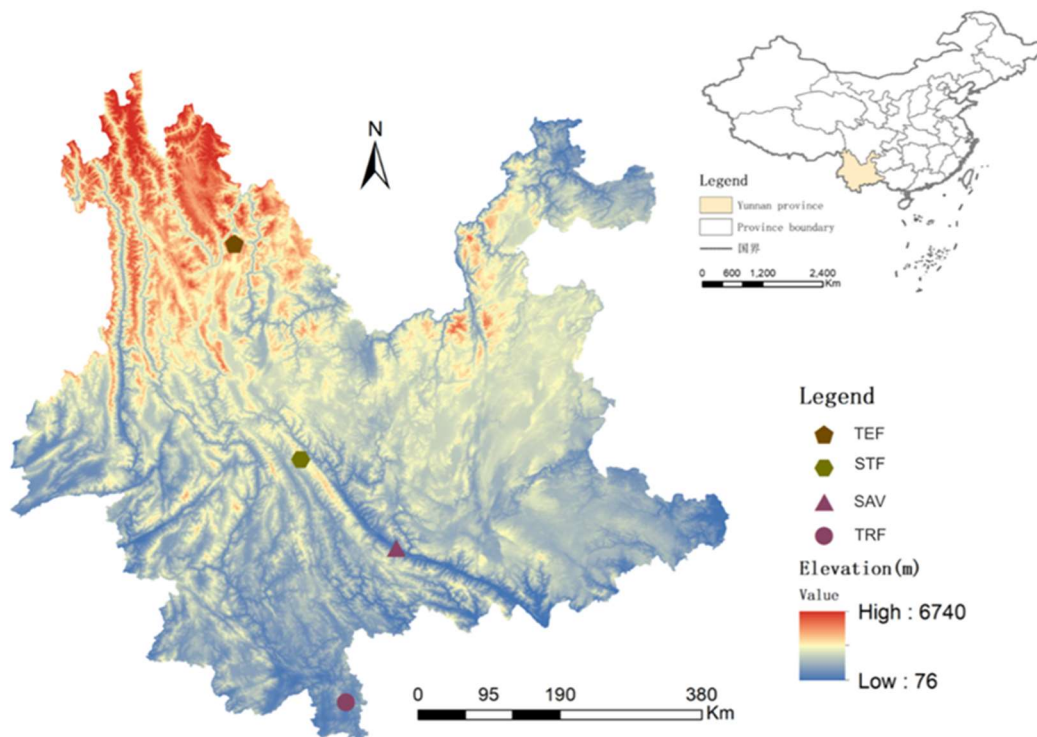


Figure 1 Site distribution.

147 We selected four vegetation types from the south to the north of Yunnan province,  
148 China, including a savanna woodland (SAV), a tropical rain forest (TRF), a  
149 subtropical broad-leaved forest (STF), and a temperate mixed forest (TEF) (Table 1  
150 and Fig. 1). Four dominant upper canopy species were chosen in each site. These  
151 species covered all the emergent species in TRF, all the canopy species in TEF, the  
152 most abundant three species and the sixth most abundant canopy species in STF, and  
153 the most abundant three species and the seventh most abundant species that grow



154 closely and under similar micro-habitat in SAV. Considering data balance across sites,  
155 the replicate individuals were determined by the species with the smallest number of  
156 individuals, thus three individuals were selected for each species. Detailed  
157 information of the species can be found in Table S1.

### 158 **Measurement of thermal regulation strategies**

159 The 3-T method was used to measure thermal regulation strategies. This method  
160 needs three temperatures: leaf temperature ( $T_l$ ), leaf temperature of non-transpiring  
161 leaf ( $T_n$ ), and air temperature ( $T_a$ ). The thermal effect of transpiration was calculated  
162 by  $T_l - T_n$  (Gates, 1968), and thermal effect of leaf physical traits compared with air  
163 was calculated by  $T_n - T_a$ . Note that transpirational cooling refers to  $T_n - T_l$ , which  
164 is therefore positive when there is a cooling effect. All the temperatures were  
165 measured by T-type thermal couples (TT-T-30-SLE-1000, OMEGA, USA; diameter  
166 = 0.25mm). To guarantee the accuracy of temperature measurements, we compared  
167 leaf temperature difference ( $dT$ ) between thermal couple and PT-100 (YAGEO  
168 Nexensos GmbH, Germany) in the field. PT-100 is a platinum resistance temperature  
169 detector (RTD) that utilizes the electrical resistance of platinum to measure  
170 temperature. The accuracy of PT-100 is reported drift of 0 °C is 0.04% (0.16 °C) after  
171 1000 hours at 400 °C in the field. The results showed thermocouple temperature  
172 measurements are slightly higher, with an average  $dT$  of 0.6%. The maximum  $dT$   
173 reached 2.7% which happened after noon (Notes S3). Temperatures were recorded by  
174 data logger (UX-120-04, HOBO, USA) every one minute from May 13 to May 16 at  
175 TRF, May 19 to May 23 at STF, May 25 to May 28 at SAV, June 4 to June 7 at TEF

176 in 2019. This period was the most severe heatwave in Yunnan province from 1961 to  
177 2019 (Kitudom *et al.*, 2022). At TRF and STF, crowns were accessed using canopy  
178 crane infrastructure, whereas at the lower canopy sites SAV and TEF, they were  
179 accessed from the ground or using a ladder. We used heat-conducting glue to fix the  
180 thermal couple head on the adaxial side of the leaves. With this method, thermal  
181 couples can be tightly fixed on leaves without impacting on stomata conductance and  
182 avoid irradiation effects on the sensor head (Kitudom *et al.*, 2022). We put Vaseline  
183 on the abaxial side of leaves to get non-transpiring leaves (all the leaves are  
184 hypostomatous) (Gates, 1968; Jones, 1999). A thin layer of Vaseline on the abaxial  
185 side of the leaf had negligible impacts on leaf physical thermal effects ((Thorpe and  
186 Butler, 1977); Notes S1 and S2 for experimental tests and sensitivity analysis of the  
187 impact of the Vaseline application). Temperatures of four mature, sun-exposed and  
188 healthy control leaves, and two non-transpiring leaves of similar traits to the control  
189 leaves were measured. Air temperatures beside these leaves were measured  
190 simultaneously with thermal couples on the abaxial sides of leaves to avoid direct  
191 solar radiation. Ten-minute average temperatures were used for analysis.  $T_n$  might be  
192 lower than  $T_l$  due to water adhering to the Vaseline surface. This situation often  
193 happened at night and in the early morning. However,  $T_n < T_l$  also occasionally  
194 happened during daytime in TEF, which might be because of weak transpirational  
195 cooling. Therefore, a small change of leaf angle, wind and radiation loading of the  
196 non-transpiring and the control leaf could induce negative  $T_n - T_l$ . We assumed  
197 transpirational cooling was zero ( $T_n = T_l$ ) when  $T_n < T_l$ .

198 **Leaf traits measurement**

199 We selected leaf traits that might be related to leaf temperature including  
200 morphological, optical, anatomical, physiological traits and material properties (Table  
201 2). Leaves for morphological traits measurement were collected adjacent to the leaves  
202 for temperature measurements for 8–10 leaves per individual and 3 individuals per  
203 species. All the leaves were scanned on a flatbed-scan scanner. Leaf area (Area), leaf  
204 perimeter (P), perimeter/area ratio (P/A), leaf length (Length), and leaf width (Width)  
205 were analyzed by ImageJ 1.52q based on the scanned image. Leaf angle was  
206 measured using the “Measure” app on Apple’s iPhone (Apple Inc.). The horizontal  
207 position is set at 0 degrees, with the leaf facing downwards, the angle is negative, and  
208 the angle is positive when the leaf is facing upwards. Ten leaves of each individual  
209 were used to measure reflectivity (R), transmissivity (T), and absorptivity (A) at  
210 wavelength between 400nm and 700nm with an integrated sphere connected to a  
211 spectrometer (USB2000, Ocean Optics, USA), and greenness with a chlorophyll  
212 meter (SPAD-502, Minolta, Japan). Leaf water content (WC) and leaf density was  
213 measured by weighing 3–8 leaves (more leaves for low-weight leaves) for each  
214 individual. WC was calculated by the ratio of weight difference between fresh and dry  
215 leaves to the dry mass (Pérez-Harguindeguy et al., 2013). Leaf fresh mass density  
216 (Density.f) and leaf dry mass density (Density.d) were calculated as the ratio of leaf  
217 fresh and dry mass to leaf volume respectively (Pérez-Harguindeguy et al., 2013).  
218 Leaf volumes were determined by the water displacement method. Four leaves of  
219 each individual were used to measure anatomical traits. Leaf thickness (Thickness),

220 the thickness of upper and lower epidermis (Epidermis\_up, Epidermis\_low), palisade  
221 mesophyll (Thickness\_palisade) and spongy mesophyll (Thickness\_spongy) were  
222 measured using paraffin cross section. Paradermal sections were cut from the middle  
223 part of the leaf avoiding major veins. Paradermal sections for stomata measurement  
224 were boiled in water for 10–15 min, then immersed in a 1:1 mixture of 30% H<sub>2</sub>O<sub>2</sub> and  
225 glacial acetic acid aqueous solution until being soft and disintegrated, after which we  
226 carefully separated the epidermis. Paradermal sections for vein analysis were  
227 bleached with 5% NaOH until they became transparent. Paradermal sections for  
228 stomata and vein analysis were stained in 1% safranin diluted with ethanol for 15 min  
229 before taking photos under a light microscope. Stomatal density was calculated by the  
230 number of stomata divided by the area of view. Vein density was calculated by the  
231 total length of veins per area. Diurnal patterns in transpiration rate, photosynthesis  
232 rate, and stomatal conductance were measured with a Portable Photosynthesis system  
233 (LI-6400, LICOR, USA) using a transparent leaf chamber. Temperature, light,  
234 relative humidity and CO<sub>2</sub> concentration during the measurements were maintained at  
235 ambient conditions (Fig. S1) and not controlled. The flow rate was 500  $\mu\text{mol}\cdot\text{s}^{-1}$ . For  
236 each individual, three leaves next to the leaves for temperature measurements, were  
237 measured repeatedly from morning to afternoon depending on solar radiation and the  
238 availability of the canopy crane at each site (SAV: 8:00–17:00; TRF: 9:20–14:40;  
239 STF: 9:30–16:30; TEF: 8:30–17:40). Gas exchange measurements were conducted for  
240 two days in SAV, STF and TEF, and one day in TRF due to the unavailability of the  
241 canopy crane. The maximum transpiration rate ( $Tr_{\text{max}}$ ), photosynthesis rate ( $A_{\text{max}}$ ) and

242 stomatal conductance ( $g_{\max}$ ) were extracted from the diurnal measurements of leaf gas  
243 exchange. These physiological traits might change with environment of measurement,  
244 while the trend among species should be stable. Photosynthetic thermal tolerance was  
245 measured with a PlanTherm PT100 (PSI, Czech Republic) based on the response of  
246 basal chlorophyll *a* fluorescence to temperature ( $F_o$ -T curve) with three sun leaves for  
247 each individual (details can be found in Kitudom et al., 2022). Leaf segments (2cm×  
248 1cm) were heated by water bath from 25 °C to 70 °C. Heating rate was 2 °C min<sup>-1</sup>.  
249  $T_{\text{crit}}$  was calculated as the intersection of lines extrapolated from the slow and fast  
250 rising portions of  $F_o$ -T curve (Knight and Ackerly, 2002).

### 251 **Meteorological measurements**

252 Meteorological data were obtained from the measurements on towers above the  
253 canopy in SAV, TRF, and STF. Meteorological data of TEF were obtained from a  
254 weather station installed in the open land at a distance of 10 meters from the forest.  
255 Air temperature, relative humidity, wind speed, and downward solar radiation (DR)  
256 were sampled at 0.5 Hz using CR1000 dataloggers (Campbell Scientific, Inc, USA) at  
257 each site. Ten-minute averages were used in the present study. The details of  
258 mounting heights and instruments are shown in table S2.

### 259 **Data analysis**

260 Individual tree averages of leaf temperature, leaf thermal effects and leaf traits were  
261 used for analysis. Considering that transpirational cooling only happened during  
262 daytime and the variance of nighttime physical thermal effects were small among  
263 species in each site and nighttime cooling is more effected by environmental factors

264 and canopy characteristics rather than physiological processes of plants, the following  
265 analysis only used daytime values ( $DR > 100 \text{ w}\cdot\text{m}^{-2}$ ).

266 • Patterns of parameters across biomes

267 Differences in leaf temperature, thermal effects of leaf physical traits and  
268 physiological traits, and leaf traits among sites were analyzed by multiple  
269 comparisons of least significant difference (LSD) (Steel et al., 1997).

270 • Leaf thermal response type

271 We calculated  $\beta$  as the slope of the regression line between  $T_a$  and  $T_l$  for each species.  
272 We then used the “slope. Test” function in R package “smart” to test the difference  
273 between  $\beta$  and 1. A  $\beta$  value is significantly smaller than 1 ( $P < 0.05$ ) indicates  
274 limited homeothermy;  $\beta$  that is not significantly different from 1 ( $P > 0.05$ ) indicates  
275 poikilothermy; and if  $\beta$  is significantly larger than 1 ( $P < 0.05$ ), this species exhibits  
276 megathermy.

277 • The relationship between thermal adaptation strategies

278 We used Pearson correlation to analyze the relationships between leaf temperature  
279 regulation strategies (transpirational cooling and physical warming during daytime)  
280 and photosynthetic thermal tolerance.

281 • The impact of microclimate and leaf traits on thermal regulation strategies

282 To analyze the different impacts of climate on leaf temperature regulation, the  
283 correlations between leaf temperature metrics ( $T_l$ ,  $dT$ , physical warming effect, and  
284 transpirational cooling) and climate parameters ( $T_a$  and  $DR$ ) were calculated using  
285 Spearman’s rank correlation. Here,  $dT$  is the temperature difference between leaf and

286 air. Correlation coefficients were expressed as  $r.Tl\_Ta$ ,  $r.Tl\_DR$ ,  $r.dT\_Ta$ ,  $r.dT\_DR$ ,  
287  $r.physic\_Ta$ ,  $r.physic\_DR$ ,  $r.trans\_Ta$  and  $r.trans\_DR$ , which were put into a PCA.  
288 This separated species out according to their relationships between leaf temperature  
289 metrics with  $Ta$  and  $DR$ , and allowed us to analyze which of these relationships are  
290 most important for this separation. This was performed using the “prcomp” function  
291 in base R. We further assessed how the position of the species is related to the species’  
292 traits. This was performed using “env\_fit” in the “vegan” package.

293 To identify key traits related to transpirational cooling and physical warming  
294 during daytime ( $DR > 100 \text{ w}\cdot\text{m}^{-2}$ ), Bayesian mixed effects models were used. For the  
295 model examining the relationship between the maximum transpiration rate and  
296 transpirational cooling (trans), the fixed effect was the maximum transpiration rate  
297 ( $Tr_{max}$ ) and the random effects were site and species (Eq. 1).

$$298 \quad \text{trans} = Tr_{max} + 1|\text{Site} + 1|\text{Species} \quad (1)$$

299 In the model exploring the relationship between the physical traits and physical  
300 warming (physic), many physical leaf traits could impact physical warming. To avoid  
301 high correlated traits in the regression model, these traits were categorized into four  
302 groups: morphological traits, optical traits, material properties, and anatomical traits.  
303 Pearson correlation was used to identify which traits that had significant correlations  
304 with leaf physical warming. The traits with the strongest or significant correlations  
305 with physical warming in each group were selected. We further checked collinearity  
306 among these traits using pairwise Pearson correlation. If the correlation coefficient  
307 was higher than 0.7, one of the two traits was removed. The retained leaf traits (Angle,

308 P, Greenness, WC, Density.d, Vein density and Palisade) were set as fixed effects for  
309 the full model (Eq. 2), with site and species serving as random effects. The fixed  
310 effects were center scaled to a mean of 0 with standard deviation of 1. According to  
311 the correlation between leaf angle and physical warming, the absolute values of leaf  
312 angle had a higher correlation with physical warming, therefore we used the absolute  
313 values of leaf angle.

$$314 \text{ physic} = |\text{Angle}| + \text{P} + \text{Greenness} + \text{WC} + \text{Density.d} + \text{Vein density} + \text{Palisade} + \\ 315 \quad 1|\text{Site} + 1|\text{Species} \quad (2)$$

316 We constructed linear mixed regression models in a Bayesian framework using R  
317 package “brms” (Burkner, 2017). We fit models with student\_t priors for all the  
318 coefficients, because the sample size was small and the population variance was  
319 unknown. Four Markov Chain Monte Carlo (MCMC) chains were used to sample  
320 from the posterior distribution of the regression parameters for each model, with 3000  
321 iterations per chain. Half of the iterations were used for warming up. Chains  
322 convergence was diagnosed by Rhat values equal to 1. For the full model of the  
323 association of leaf physical traits to physical warming, no coefficient was significant.  
324 To identify the best model, we dropped traits from the full model one by one, and  
325 used WAIC values for model selection. Conditional  $R^2$  and Marginal  $R^2$  were  
326 calculated using the  $r^2$  function in the “performance” R package (Lüdtke et al.,  
327 2021). Effect size was calculated by the following equation (Le Provost et al., 2020):

$$328 \text{ Effect size} = \frac{\alpha_i}{\sum_1 \alpha} mR^2 \quad (3)$$



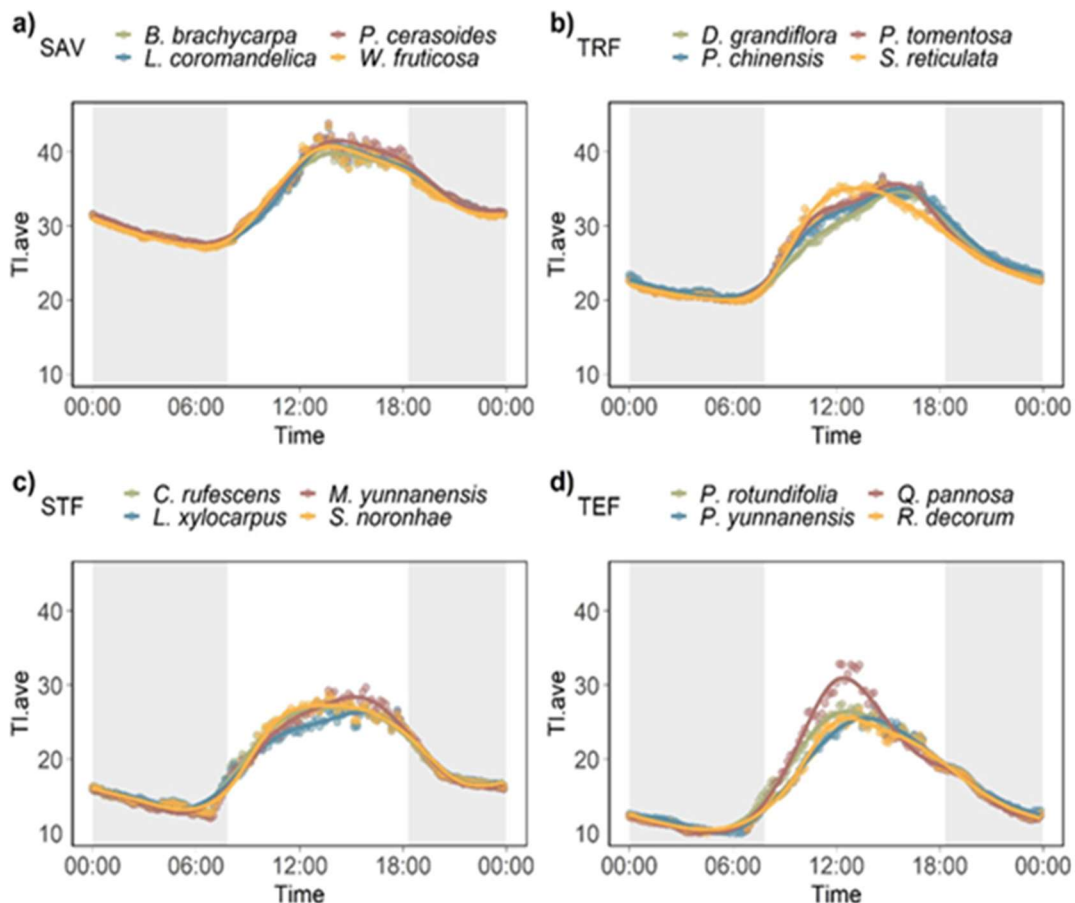
329 Where  $\alpha_i$  is the coefficient of the fixed effect  $i$ ,  $mR^2$  is the marginal  $R^2$  of the model. If  
 330 the model had no random effects,  $mR^2$  equals the  $R^2$  of the model.

331 We found a non-linear relationship between leaf area and leaf physical  
 332 warming. To investigate this relationship, we separately analyzed two ranges of leaf  
 333 area ( $< 50 \text{ cm}^2$  and  $\geq 50 \text{ cm}^2$ ) using Pearson correlation. In addition, we employed  
 334 Pearson correlation was used to examine the relationship between leaf traits and  
 335 microclimate parameters with leaf physical warming at each site. Correlations were  
 336 considered significant at  $P < 0.05$ .

337

## 338 RESULTS

### 339 Leaf temperature patterns across and within sites



340

Figure 2 Diurnal leaf temperatures (10 min average). Shading areas indicate nighttime. SAV, savanna woodland; TRF, tropical rain forest; STF, subtropical evergreen broad-leaved forest; TEF, temp mixed forest.

341 Leaf temperatures increased from TEF to SAV. The minimum leaf temperatures  
 342 ranged from  $8.4 \pm 0.11$  °C in TEF to  $26.2 \pm 0.11$  °C in SAV. The maximum leaf  
 343 temperatures ranged from  $33.3 \pm 2.07$  °C in TEF to  $46.0 \pm 0.51$  °C in SAV (Table 3).  
 344 Daily leaf temperature ranges of TRF and TEF species were higher than STF and  
 345 SAV species ( $P = 0.003$ ). Of all the species, *Q. pannosa* in TEF had the highest daily  
 346 leaf temperature range ( $25.9 \pm 1.85$  °C), and *B. brachycarpa* in SAV had the lowest  
 347 daily leaf temperature range ( $16.4 \pm 0.52$  °C) (Fig. 2). The maximum leaf

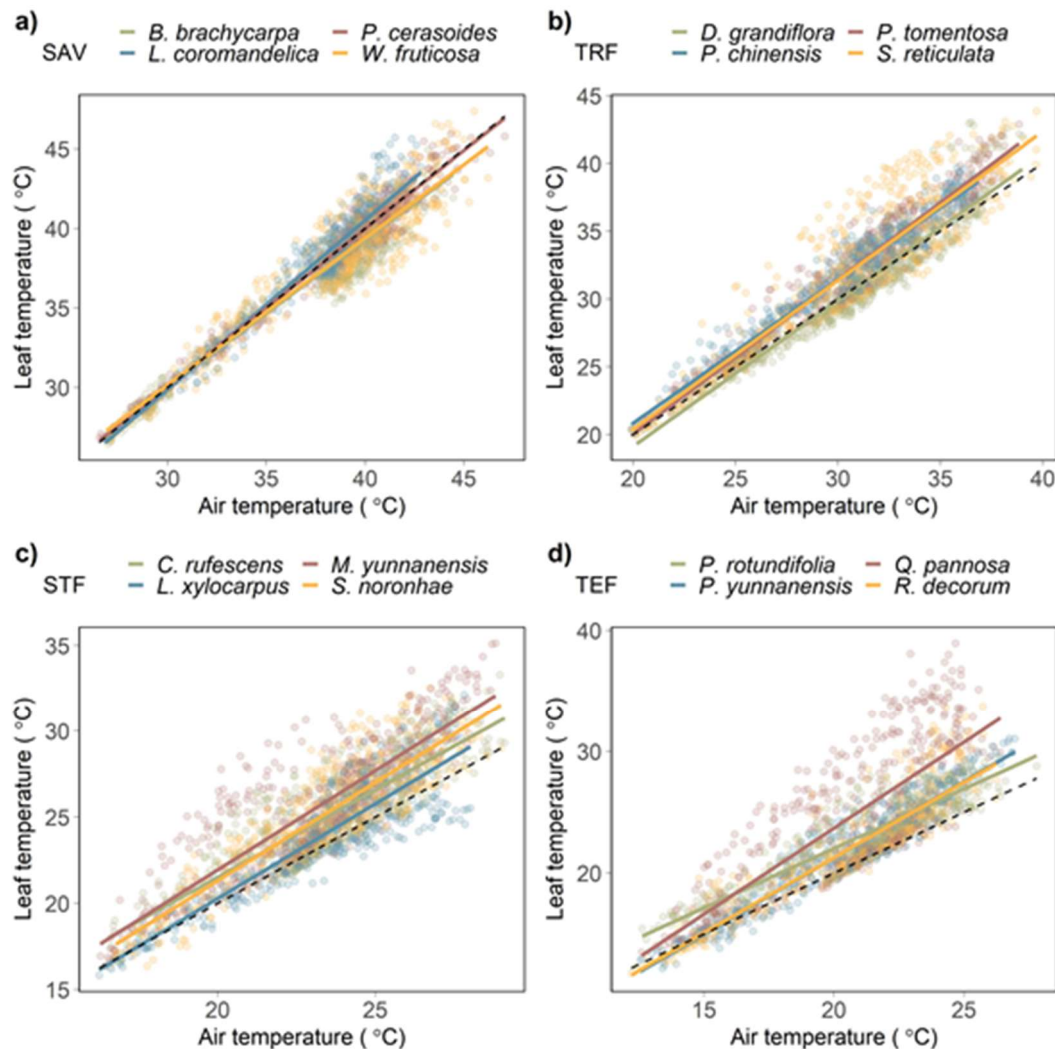


Figure 3 Linear regression between air temperature and leaf temperature. The slope of the dashed line is 1. SAV, savanna woodland; TRF, tropical rain forest; STF, subtropical evergreen broad-leaved forest; TEF, temperate mixed forest.

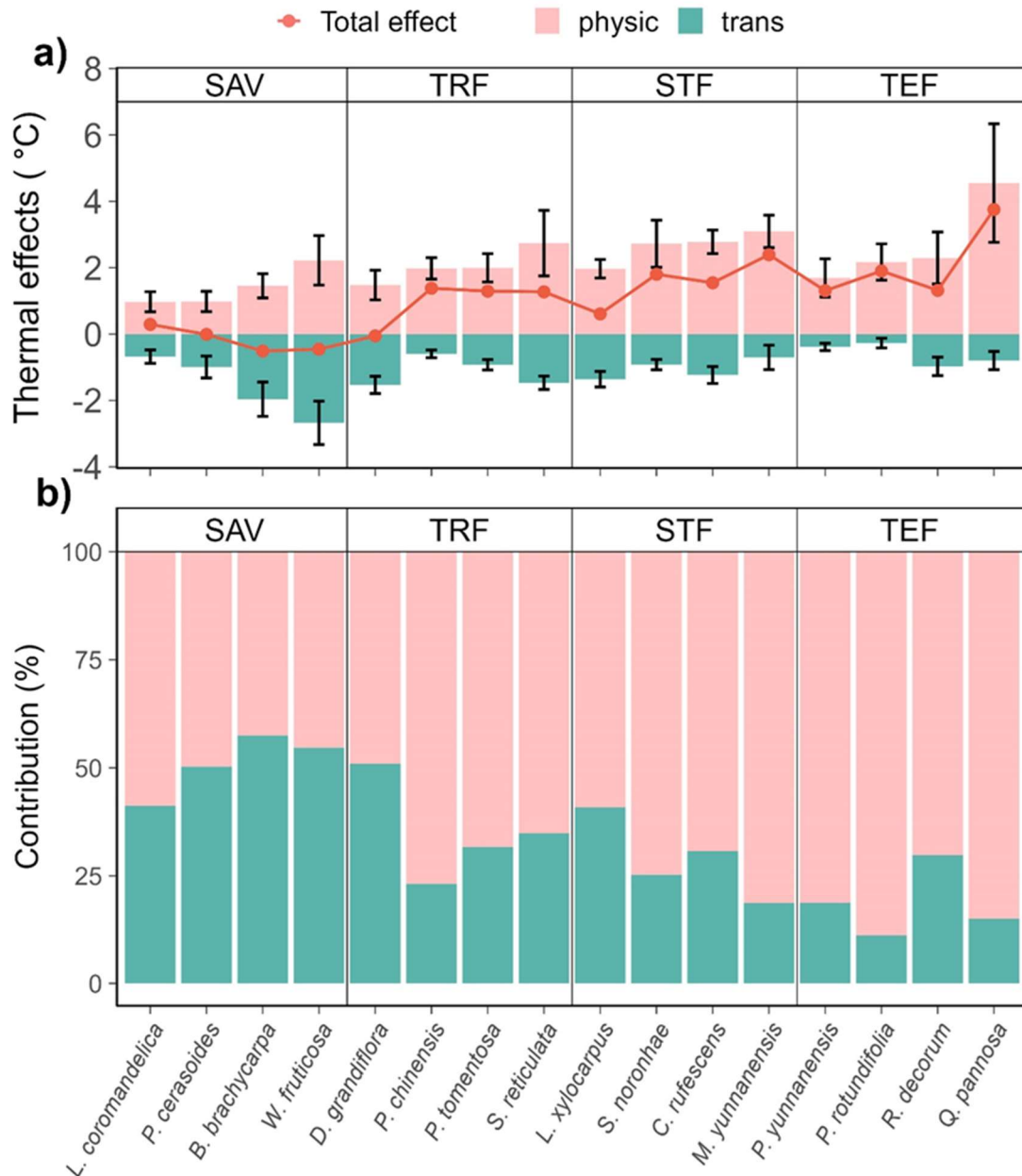
348 temperatures also varied among species within sites. Within each site, the maximum  
349 leaf temperature variances among species were 1.2 °C, 1.8 °C, 2.9 °C and 13.6 °C in  
350 SAV, TRF, STF, and TEF respectively.

351 Leaf temperatures of SAV species were closest to air temperature. Site mean  
352 temperature difference between leaf and air (dT) decreased with site mean  
353 temperature ( $P < 0.001$ ) (Table 3). SAV species *P. cerasoides* and *W. fruticosa*  
354 exhibited poikilothermic characteristics ( $\beta = 1$ ); SAV species *B. brachycarpa* showed  
355 limited homeothermy ( $\beta < 1$ ); and all the other species displayed megathermy ( $\beta > 1$ )  
356 (Fig. 3). Although  $\beta$  of TEF species *P. rotundifolia* was below 1, its leaf temperatures  
357 were consistently higher than air temperature.

### 358 **Thermal regulation strategies across and within sites**

359 Compared with air temperature, physical traits had warming effects on leaves during  
360 daytime and cooling effects during nighttime (Fig. S2). All the species showed the  
361 strongest transpirational cooling before or around the time of peak air temperature,  
362 except for *L. coromandelica* in SAV (Fig. S3). The physical daytime warming and  
363 nighttime cooling effects were positively correlated across sites (Pearson correlation =  
364 0.74,  $P = 0.001$ ), however nighttime cooling was very weak and differences among  
365 species were small. Thus, the following analysis only includes physical warming and  
366 transpirational cooling during daytime ( $DR > 100 \text{ w}\cdot\text{m}^{-2}$ ). Generally, the plants in the  
367 hotter sites exhibited stronger transpirational cooling and less physical warming. For  
368 three of the SAV species (*B. brachycarpa*, *W. fruticosa*, and *P. cerasoides*) and one  
369 TRF species (*D. grandiflora*), the main thermal regulations were transpirational

370 cooling. Among them, *B. brachycarpa* and *W. fruitcosa* had the strongest  
371 transpirational cooling of all the species (Fig. 4a). In contrast, the species in the cold  
372 sites tended to have limited transpirational cooling, with *P. rotundifolia* and *P.*  
373 *yunnanensis* in TEF forest showing the weakest transpirational cooling. Physical  
374 warming dominated thermal regulation strategies for the species in TRF, STF and  
375 TEF, except for *D. grandiflora* in TRF (Fig. 4a). The contribution of physical  
376 warming to thermal regulation increased from the hot sites to the cold sites. TEF  
377 species *Q. pannosa* had the strongest physical warming (Fig. 4b).



378

Figure 4 Leaf temperature regulation strategies. a). Thermal effects of transpiration and leaf physical traits during daytime; b). The contribution of transpirational cooling and leaf physical warming to the temperature difference between leaf and air. SAV, savanna woodland; TRF, tropical rain forest; STF, subtropical evergreen broad-leaved forest; TEF, temperate mixed forest.

379 **The impact of microclimate and leaf traits on thermal regulation strategies**

380 The correlation of leaf temperature metrics (Tl, dT, transpirational cooling, and

381 physical warming) with Ta and DR separated species out. PC1 explained 39% and

382 PC2 explained 29% of the variance. PC1 was dominated by the positive relationship  
383 between Tl and DR, and the negative relationships between transpirational cooling  
384 and both Ta and DR. Species with high scores on this axis (*P. rotundifolia*, and *M.*  
385 *yunnanensis*) had stronger positive relationships of Tl with DR, dT with Ta and DR,  
386 and negative relationship of transpirational cooling with Ta and DR, hence displayed  
387 less transpirational cooling and high leaf temperature under hot and bright conditions.  
388 Species with low scores on this axis (*P. cerasoides*, *W. fruticosa*, and *B. brachycarpa*)  
389 had stronger positive relationships of transpirational cooling with Ta and DR, and  
390 therefore displayed stronger transpirational cooling under hot and bright conditions,  
391 and accordingly, the leaf temperature did not increase strongly under increasing light  
392 intensity. PC2 was dominated by the positive relationship between physical warming  
393 and DR. The species with high scores on this axis (*P. tomentosa*, and *P. chinensis*) had  
394 stronger positive relationships between physical warming and DR, therefore displayed  
395 more physical warming under bright conditions. Species with low scores on this axis  
396 (*P. rotundifolia*, and *L. xylocarpus*) showed weaker positive relationships between  
397 physical warming and DR, therefore displayed less physical warming compared with  
398 other co-existing species under bright conditions (Fig. 5).

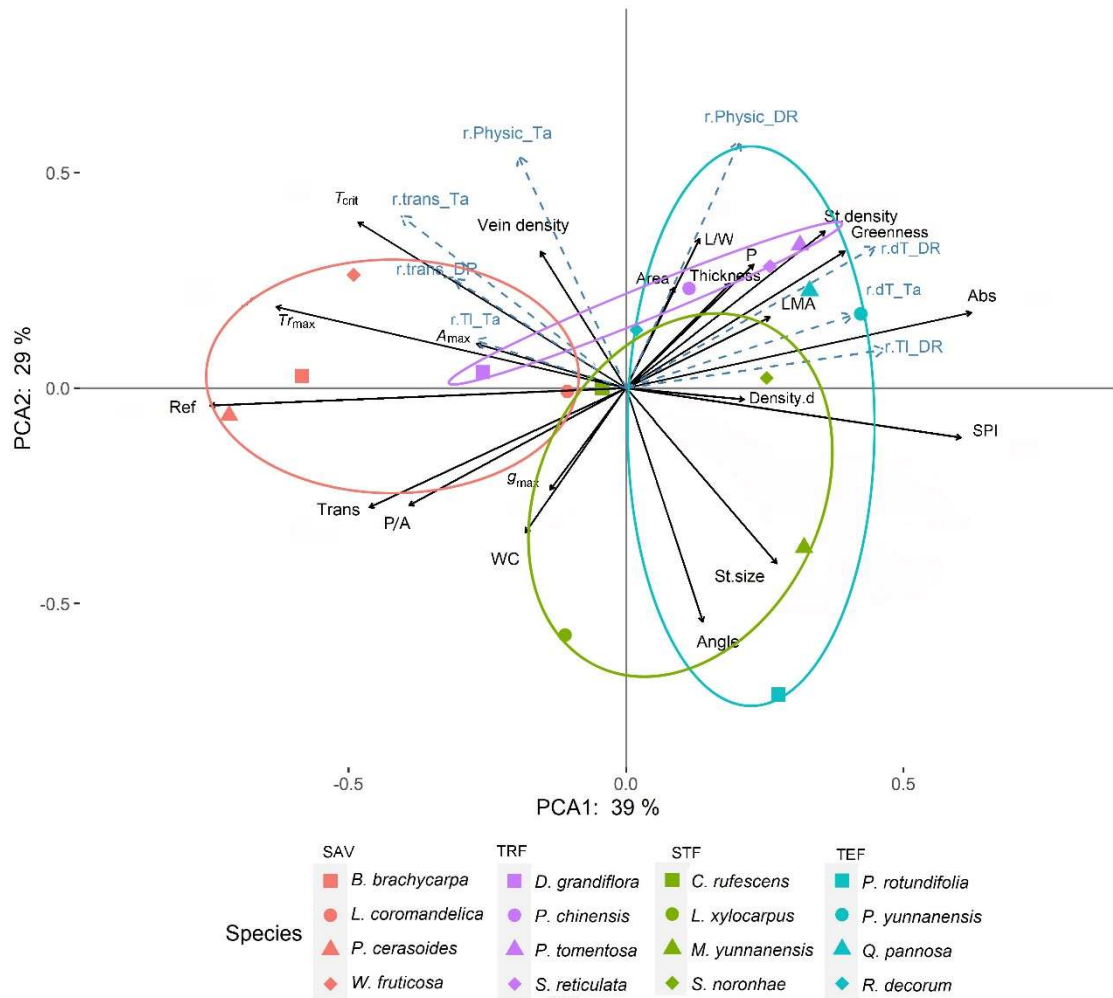


Figure 5 Principal component analysis of the relationship between thermal regulation strategies and climate factors and leaf traits.  $r.trans\_DR$ , Pearson correlation coefficient between transpirational cooling and downward solar radiation (DR);  $r.trans\_Ta$ , Pearson correlation coefficient between transpirational cooling and air temperature (Ta);  $r.physic\_DR$ , Pearson correlation coefficient between physical warming and DR;  $r.physic\_Ta$ , Pearson correlation coefficient between physical warming and Ta;  $r.dT\_Ta$ , Pearson correlation coefficient between temperature difference between leaf and air (dT) and Ta;  $r.dT\_DR$ , Pearson correlation coefficient between dT and DR;  $r.Tl\_DR$ , Pearson correlation coefficient between leaf temperature (Tl) and DR;  $r.Tl\_Ta$ , Pearson correlation coefficient between Tl and Ta. SAV, savanna woodland; TRF, tropical rain forest; STF, subtropical evergreen broad-leaved forest; TEF, temperate mixed forest.

400 With reference to plant traits, PC1 was dominated by gas exchange. Species with low  
 401 values canceled out their heating with transpirational cooling (Fig. 4b), potentially  
 402 giving them a photosynthetic advantage. These species also had high reflectance. PC2  
 403 was positively related to leaf size (Area and L/W), greenness and stomatal density,  
 404 while negatively related to WC and  $g_{\max}$  (Fig.5). Therefore, large leaves had stronger  
 405 physical warming under bright conditions, however, this warming effect can be  
 406 balanced by WC. The maximum stomatal conductance was coupled with leaf shape  
 407 and water content (Fig. 5).

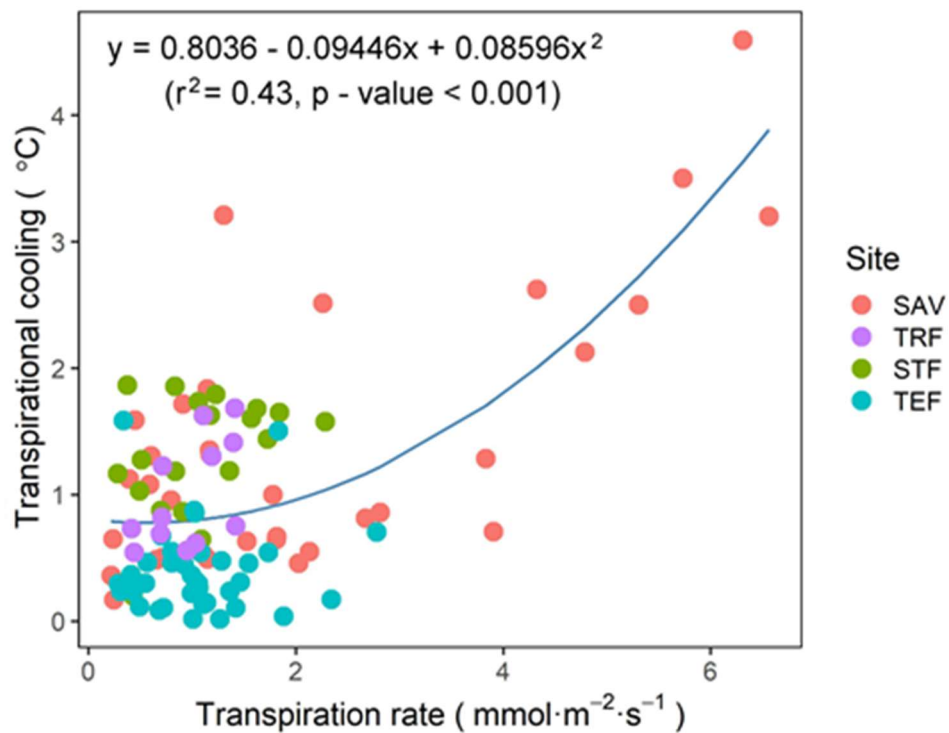


Figure 6 The relationship between transpirational cooling and transpiration rate. SAV, savanna woodland; TRF, tropical rain forest; STF, subtropical evergreen broad-leaved forest; TEF, temperate mixed forest.

408 Bayesian linear mixed regression showed that the marginal  $R^2$  between the  
 409 maximum transpiration rate and transpirational cooling was 0.461. Instantaneous



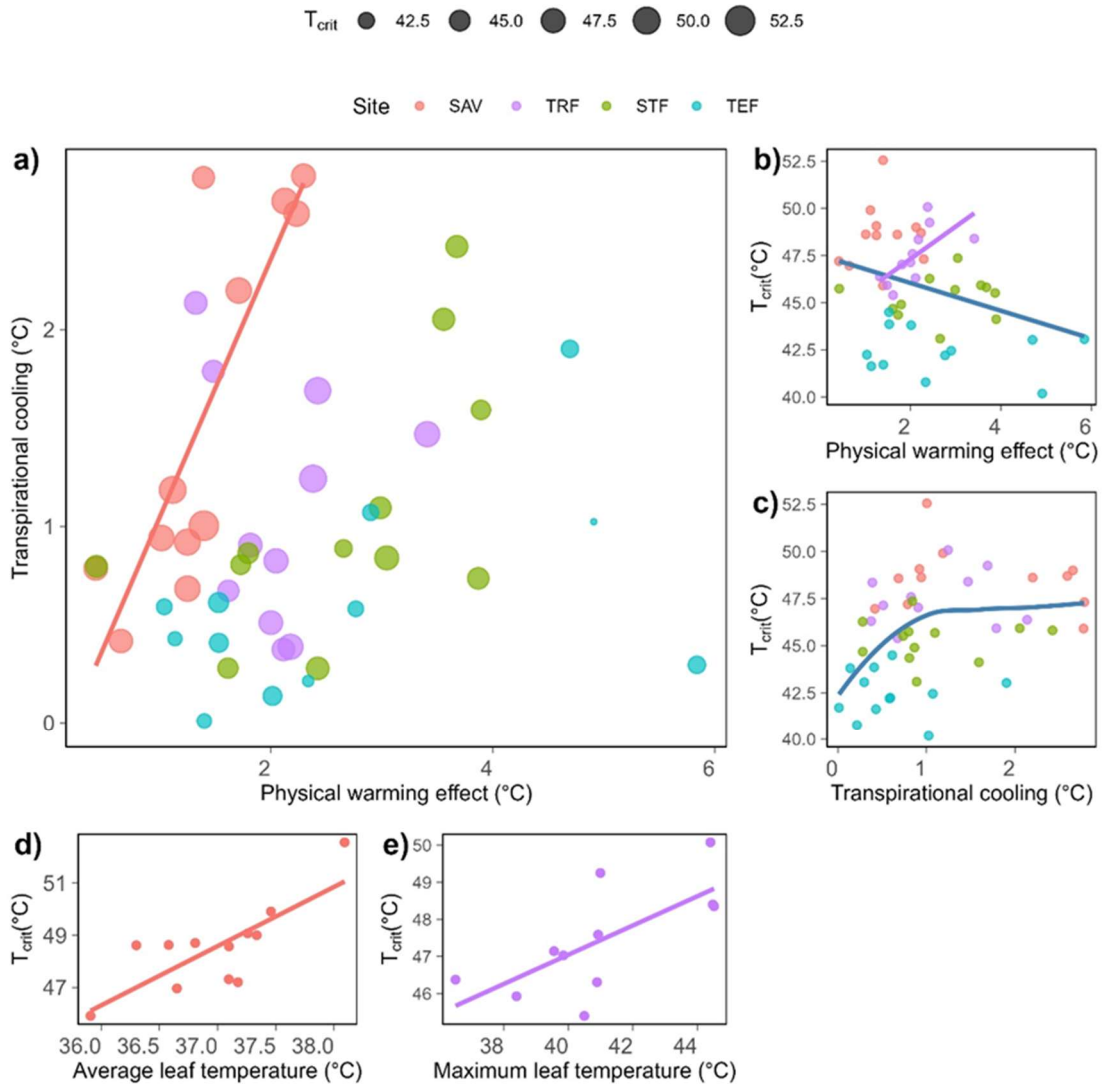
410 transpiration rates and transpirational cooling presented a quadratic relationship,  
411 however, the relationship was weak when the transpiration rate was below 2.5  
412  $\text{mmol}\cdot\text{s}^{-1}\cdot\text{m}^{-2}$  (Fig. 6). The best Bayesian mixed regression model showed that only  
413 WC or Angle had significant negative relationships with physical warming effects,  
414 with a marginal  $R^2$  0.213 and  $R^2$  0.114 respectively. There was a significant positive  
415 correlation between leaf areas and physical warming effects for leaves smaller than 50  
416  $\text{cm}^2$  (Pearson correlation = 0.52,  $P = 0.005$ ), whereas the correlation turned negative  
417 for leaves larger than 50  $\text{cm}^2$  (Pearson correlation = -0.74,  $P = 0.03$ ).

418         The leaf traits and microclimate parameters that had high correlation with leaf  
419 physical warming differed among sites. The significantly correlated leaf traits and  
420 microclimate parameters were WC, optical traits (Trans, Ref, Abs and Chl),  
421 physiological traits ( $Tr_{\max}$ ,  $A_{\max}$ , and  $g_{\max}$ ), Vein density and  $Ta_{\max}$  in SAV; WC, L/W,  
422 leaf physiological traits ( $Tr_{\max}$ ,  $A_{\max}$ , and  $g_{\max}$ ,  $T_{\text{crit}}$ ), Epidermis\_up, and  $Ta_{\max}$  in TRF;  
423 leaf material property (density.d and WC) and SPI in TEF. No significant correlations  
424 between leaf traits and microclimate parameters and leaf physical warming were  
425 found in STF (Fig. S4).

#### 426 **The relationship between thermal adaptation strategies**

427 Transpirational cooling and physical warming effects showed positive correlation  
428 across sites, but these correlations were significant only for SAV species within sites  
429 (Pearson correlation = 0.96,  $P = 0.04$ ) (Fig. 7a). Thermal tolerance was negatively  
430 correlated with physical warming effects across sites (Pearson correlation = - 0.31,  $P$   
431 = 0.03), while a significant positive correlation was found for TRF species (Pearson

432 correlation = 0.67,  $P = 0.02$ ) (Fig. 7b). Photosynthetic thermal tolerances increased  
 433 with transpirational cooling, asymptoting when thermal tolerance reached 46 °C (Fig.  
 434 7c). All four SAV species were deciduous, and shed leaves during dry season, which  
 435 enables them to avoid heat stress when water is limited. Therefore, thermal regulation,  
 436 thermal tolerance and thermal avoidance support thermal adaptation of SAV species  
 437 together. In the two hot forests, thermal tolerance was positively correlated to leaf  
 438 temperature (Pearson correlation = 0.77,  $P = 0.003$  in SAV, and Pearson correlation =  
 439 0.7,  $P = 0.02$  in TRF) (Fig. 6d-e).



440

Figure 7 The relationship between thermal adaptation strategies.  $T_{crit}$ , photosynthetic thermal tolerance; SAV, savanna woodland; TRF, tropical rain forest; STF, subtropical evergreen broad-leaved forest; TEF, temperate mixed forest.

441 **DISCUSSION**

442 **Thermal regulation strategies across a temperature and precipitation gradient**

443 Transpirational cooling and physical warming effects of leaves varied with vegetation  
444 types along a temperature and precipitation gradient. The first two hypotheses that  
445 leaf physical cooling dominates leaf regulation strategies for the savanna species, and  
446 that both transpirational cooling and leaf physical traits are important for leaf cooling  
447 for the tropical rain forest species, were not fully supported by our results. Instead,  
448 transpirational cooling prevailed in thermal regulation of SAV species, in addition to  
449 leaf physical traits to reduce physical warming. TRF species presented moderate  
450 transpirational cooling and physical warming. The hypotheses regarding thermal  
451 regulation strategies of STF and TEF species were supported by our results.

452

453

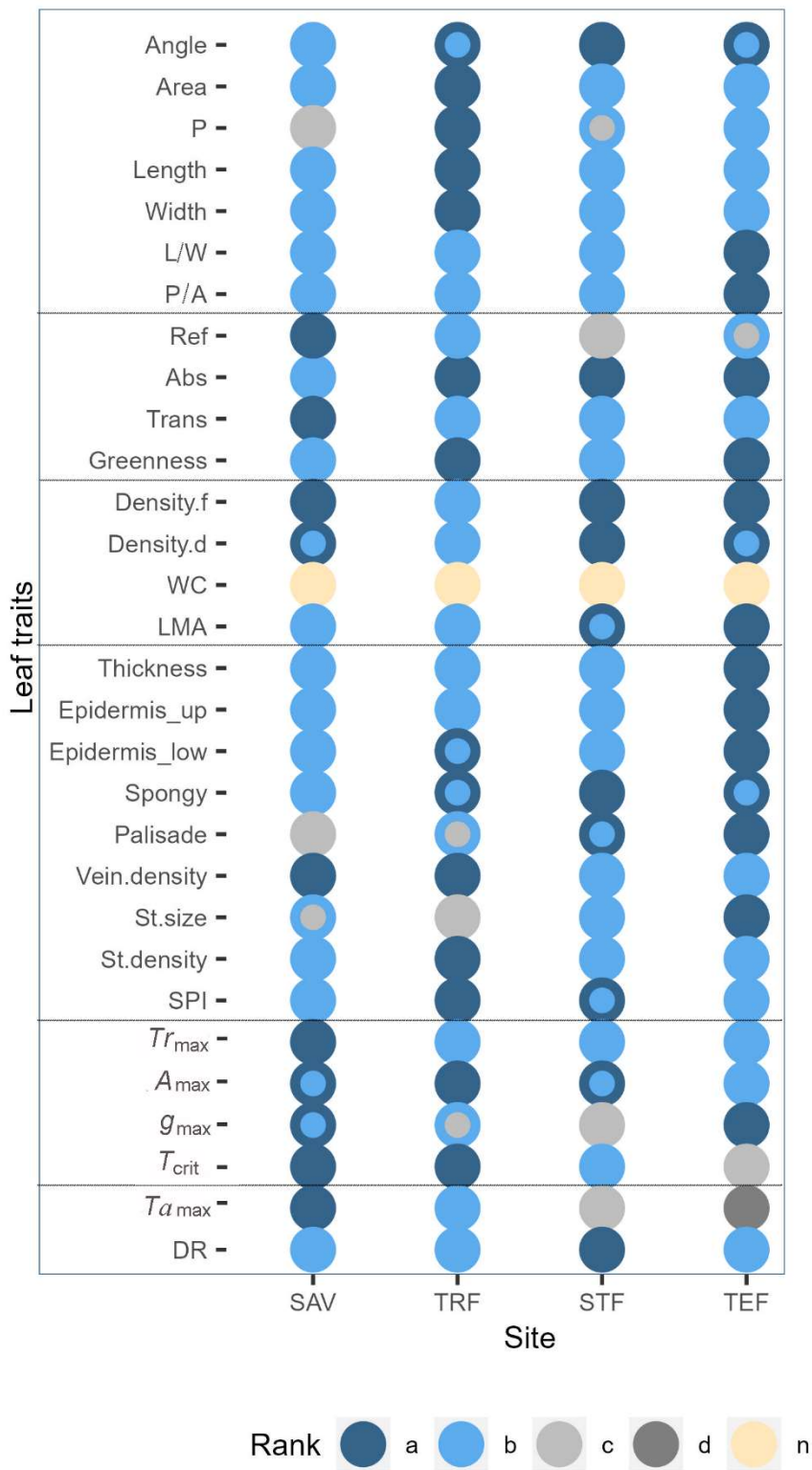


Figure 8 Multiple comparison of leaf traits and microclimate parameters among sites. SAV, savanna woodland; TRF, tropical rain forest; STF, subtropical evergreen broad-leaved forest; TEF, temperate mixed forest. Different color means significant difference. The same color means no significant difference. Values decreased from a to d.

455 The results showed that plants in the hot environment mainly relied on transpirational  
456 cooling to avoid high leaf temperatures (Fig. 4). An increasing number of studies have  
457 reported increased transpiration rates at high temperature (Crawford et al., 2012; Lin  
458 et al., 2017; Sadok et al., 2021; Slot et al., 2016; Urban et al., 2017), even under  
459 drought conditions (Aparecido et al., 2020; Smith, 1978; Urban et al., 2017).  
460 Transpirational cooling may thus be even more important in arid and hot  
461 environments due to its high cooling efficiency and its greater plasticity than leaf  
462 physical traits. High VPD in a dry environment can facilitate transpirational cooling  
463 as long as the stomata remain open. Although high thermal tolerance can partially  
464 compensate for weak transpirational cooling, we did not find this pattern in our  
465 research. On the contrary, both transpirational cooling and thermal tolerance increased  
466 with environment temperature until thermal tolerance reached a saturation point (Fig.  
467 7c). In addition, reducing physical warming is necessary for the plants in hot-dry  
468 environment. SAV species had the lowest absorptivity and the highest reflectivity (Fig.  
469 8), so that they can alleviate radiation loading, and hence showed low values of  
470 physical warming (Fig. 4a). In addition to thermal regulation, species in the hot sites  
471 (SAV and TRF) also had high photosynthetic thermal tolerance (Kitudom et al. 2022),  
472 which would enable them to operate within their thermal safety margin. Most species  
473 in SAV are deciduous species. On one hand, shedding leaves during the dry season  
474 can further avoid heat damage (Zhang et al., 2012). On the other hand, deciduous  
475 species usually had higher water and carbon exchange rate than evergreen species, so  
476 that they can grow fast during the growing season and reduce leaf temperature with

477 high transpiration rates (Tomlinson et al., 2013). This demonstrates that plants can  
478 utilize multiple methods to alleviate heat stress in extremely hot environments,  
479 therefore there is no trade-off between thermal regulation, thermal tolerance and  
480 thermal avoidance.

481 In cooler forests, the primary stress may shift from heat to other elements such  
482 as coldness, light, or herbivory. Consequently, the strategies for adapting to heat  
483 become weaker or shift towards cold adaptation. For instance, the offset of physical  
484 warming through transpirational cooling diminishes (Fig 7a), and the relationships  
485 between thermal tolerance and leaf temperatures vanish in cool forests (Fig 7d and e).  
486 TEF species have developed mechanisms to increase leaf temperature to adapt to low  
487 temperatures. Transpiration always cools leaves; generally, only leaf physical traits,  
488 except for thermogenesis, can have warming effects. Accordingly, physical warming  
489 dominated thermal regulation for the species in cold regions. Take *Q. pannosa* as an  
490 example, it has the lowest water content and high absorptivity and density, as well as  
491 being covered by dense brown trichome on the abaxial side of the leaf. As a result, *Q.*  
492 *pannosa* showed the strongest physical warming among all the species. In addition to  
493 leaf traits at the leaf level, some other traits at branch and canopy level also contribute  
494 to leaf temperature regulation. For instance, the emergent trees in TRF promote  
495 convection compared to a more even canopy; most of the TEF species have short  
496 petioles and clustered leaves, which increases the thickness of the insulating boundary  
497 layer (Michaletz and Johnson, 2006; Smith and Carter, 1988). For the species without  
498 specific traits to resist the cold, shedding leaves during winter is a final solution. The

499 ambient temperature in STF is cool, with few extreme temperatures, therefore we did  
500 not find any leaf physical trait significantly related to physical warming (Fig. S4).  
501 Even so, the dense and even canopy at STF could provide a heat buffer to extreme  
502 temperatures. In brief, plants under extreme thermal environment can utilize all means  
503 to optimize performance and survive. Integrating studies at leaf, branch and canopy  
504 levels can reveal the mechanisms for plant adaptations to the thermal environment.

### 505 **Leaf regulation strategies among species**

506 Even under the same environment, plants might adopt different leaf thermal  
507 regulation strategies. Pioneer species typically show more active metabolism (Bazzaz,  
508 1979), hence stronger transpirational cooling. In SAV, *W. fruticosa* and *B.*  
509 *brachycarpa* are shrubs. They have much higher photosynthetic and transpiration  
510 rates, shorter leaf life span (Zhang, 2007; Zhang et al., 2019) and high branch die  
511 back ratio compared with the other two tree species (Chen et al., 2021). They showed  
512 strong transpirational cooling. To balance transpirational cooling and water shortage,  
513 *W. fruticosa* develops few small leaves; *B. brachycarpa* folds leaves under strong  
514 solar radiation (Crawford et al., 2012; Lin et al., 2017). Blonder & Michaletz (2018)  
515 and Blonder et al. (2023) proposed that stomatal optimization models should consider  
516 additional optimization criteria related to avoiding thermal mortality under extreme  
517 hot environment. Generally, photosynthesis and transpiration are coupled because  
518 both CO<sub>2</sub> and water vapor enter and exit through the stomata. However, under  
519 extreme high temperature, transpiration might increase regardless of photosynthesis  
520 (Drake et al., 2018; Feng et al., 2023; Urban et al., 2017). *W. fruticosa* and *B.*

521 *brachycarpa* represented low water use efficiency when exposed to high temperatures  
522 (Fig. S5), indicating that they may adjust their stomata to prioritize leaf cooling over  
523 carbon gain. Plants from various functional groups can employ a wide range of water  
524 use strategies (Aparecido et al., 2020; Bueno et al., 2019; Gong et al., 2023). The  
525 other two SAV species adopt more conservative water use strategies. The TRF  
526 species *D. grandiflora* presented similar thermal regulation strategies to SAV species,  
527 which involve high levels of transpirational cooling. However, *D. grandiflora* showed  
528 higher water use efficiency during the daytime (Fig S5), suggesting that it may adjust  
529 its stomata to maximize carbon gain instead. This species is characterized by  
530 unusually large and evergreen leaves which had a disadvantage in heat dissipation.  
531 Nonetheless, the high transpiration rate accompanied by high photosynthesis rate and  
532 large leaves, benefit the maximization of carbon gain, enabling *D. grandiflora* to  
533 quickly reach the canopy as a pioneer tree (Mo et al., 2013). In addition, heat stress in  
534 TRF was not as strong as it is in SAV, allowing growth to be prioritized over avoiding  
535 heat stress. Although *D. grandiflora* had the largest leaf size and absorptivity, its  
536 physical warming was weakest among TRF species. Self-shading, more vertical leaf  
537 angles, and high water content might play important roles in reducing and buffering  
538 leaf temperature.

### 539 **The relationship between thermal response and thermal regulation**

540 Energy balance theory predicts that limited homeothermy ( $\beta < 1$ ) occurs when  
541 stomatal conductance is high and convective resistance is low; poikilothermy ( $\beta = 1$ )  
542 occurs when convective resistance is low; megathermy ( $\beta > 1$ ) occurs when



543 microclimate or trait parameters co-vary in certain ways with  $T_a$ , e.g. when incident  
544 radiation or relative humidity increase with  $T_a$  (Blonder and Michaletz, 2018).  
545 However, the relationships between  $\beta$  and the parameters of leaf traits and  
546 environment are too complex to be simulated by a simple model. We can evaluate  $\beta$   
547 from the perspective of thermal regulation. When transpirational cooling is stronger  
548 than physical warming, plants present homeothermy; when transpiration cooling  
549 equals physical warming, plants present poikilothermy; when transpirational cooling  
550 is weaker than physical warming, plants present megathermy. In the present study,  
551 most species were megathermic; only two poikilothermic (*P. cerasoides* and *W.*  
552 *fruticosa*) and one limited homeothermic species (*B. brachycarpa*) were found in  
553 SAV. Our results suggest that plants present limited homeothermy at the biome scale,  
554 as cooling effects were stronger in hotter environments and warming effects were  
555 stronger in colder environments. However, at the species level, megathermy is more  
556 typical for sun leaves in field conditions, which is in accordance with the finding from  
557 Blonder & Michaelletz' leaf energy balance model (Blonder & Michaelletz, 2018). A  
558 growing number of studies reports megathermy of sun leaves under sunshine (Fauset  
559 et al., 2018; Still et al., 2022). Air is almost transparent to solar radiation, while leaves  
560 can absorb more radiation than air, therefore thermal effects of leaf physical traits  
561 always have a warming effect under solar radiation, if there is convective resistance.  
562 Only when leaves are small and under strong wind, convective resistance becomes  
563 insignificant (Muller et al., 2021). However, this situation was not common under  
564 field conditions in our study. Reducing solar radiation loading is indeed another

565 mechanism to alleviate physical warming. For example, the desert plant *Welwitschia*  
566 *mirabilis* achieves relatively low leaf temperature by high reflectivity and casting  
567 shadow above the ground (Schulze et al., 1980). Although high reflectivity and low  
568 absorptivity can reduce radiation loading, these factors are unlikely to reduce  $\beta$  below  
569 1 without transpiration.

570         The limited homeothermy of *B. brachycarpa* can be a result of its high stomatal  
571 conductance and small leaves (low convective resistance), and its capacity to fold  
572 leaves to avoid radiation loading. Although *W. fruticosa* also had high stomatal  
573 conductance, its strong physical warming balanced the cooling effect of transpiration,  
574 therefore it presented poikilothermy. *P. cerasoides* and *L. coromandelica* had low  
575 absorptivity, relatively small leaves, and more vertical leaf angles which can reduce  
576 physical warming. However, transpirational cooling of *P. cerasoides* was stronger  
577 than *L. coromandelica*, thus *P. cerasoides* presented poikilothermy, while *L.*  
578 *coromandelica* presented megathermy. In TEF, wind speed was the highest among the  
579 four sites. *P. rotundifolia*, which had  $\beta < 1$ , has long petioles. They can swing with  
580 wind and leaf angle becomes steeper under high temperature, thus convection and  
581 reducing radiation loading might be the main causes of low  $\beta$  for *P. rotundifolia*.

### 582 **3-T method for studying thermal regulation**

583 The 3-T method provided an effective and convenient way to study thermal regulation  
584 strategies. It can be used to continuously monitor transpirational cooling and physical  
585 thermal effects in the field, and it enables us to disentangle the potentially interacting  
586 effects of transpiration and leaf physical traits. This method is not restricted to

587 application at the leaf level; it can also be used at the stand or community level. The  
588 development of technology for achieving non-transpiring leaves is ongoing. Coating  
589 leaves with Vaseline is a traditional way (Lin et al., 2017; Thorpe and Butler, 1977;  
590 Wallace and Clum, 1938; Zhang et al., 2020). The main artifact of Vaseline coating is  
591 the changes of the boundary layer (see Notes S1), which means that the coating must  
592 be applied thinly and evenly ( $\leq 3 \text{ mg} \cdot \text{cm}^{-2}$ ). Developing new materials and using  
593 high-precision modeling to calculate  $T_n$  can further improve the accuracy of the 3-T  
594 model.

595         There are some notes for the 3-T method. First, the leaf with Vaseline must  
596 have similar leaf physical traits to the control leaf to minimize the influence on leaf  
597 physical thermal effects; Second, if there was condensation or rain on leaves, water  
598 would be retained longer on the Vaseline surface than leaves.  $T_n$  might be lower than  
599  $T_l$  when control leaves were dry while the Vaseline coated leaves were wet; Third, the  
600 high temperature of  $T_n$  might damage leaf, the damaged leaf should be replaced in  
601 time.

## 602 **CONCLUSION**

603 The present research used 3-T method to study thermal regulation strategies of leaves  
604 along a temperature and precipitation gradient. We found higher transpirational  
605 cooling in hotter sites and stronger physical warming in cooler sites. The results  
606 highlight the key role of transpirational cooling in hot sites, even in an arid region.  
607 Although leaf physical traits can relieve heat damage, no physical traits at the leaf  
608 level can reduce leaf temperature equal to or below air temperature under solar

609 radiation. Among leaf physical traits, water content, leaf area and leaf angle play  
610 significant role in regulating leaf physical thermal effects. The present research  
611 revealed a relatively comprehensive scenario of leaf regulation strategies under four  
612 distinct environments, thereby enhance our understanding of how plants adapt to  
613 thermal environments.

614

### 615 **Acknowledgement**

616 This research is supported by the National Natural Science Foundation of China  
617 [grant number 32171504 and 31870386], ANSO Scholarship for Young Talents  
618 Award, Chinese Academy of Sciences President's International Fellowship Initiative  
619 [grant number 2016VBA036], Top young talents of Yunnan high-level talent training  
620 and support program [grant number YNWR-QNBJ-2019-191], Natural Environment  
621 Research Council [grant number NE/V008366/1], West Light Talent Program of the  
622 Chinese Academy of Sciences [xbzg-zdsys-202218] and the support of the 14th Five-  
623 Year Plan of Xishuangbanna Tropical Botanical Garden, Chinese Academy of  
624 Sciences. Thanks for the field work support from National Forest Ecosystem Research  
625 Station at Xishuangbanna, National Forest Ecosystem Research Station at Ailaoshan,  
626 Yuanjiang Savanna Ecosystem Research Station, Xishuangbanna Tropical Botanical  
627 Garden, Chinese Academy of Sciences, Lijiang Forest Biodiversity National  
628 Observation and Research Station, Kunming Institute of Botany, Chinese Academy of  
629 Sciences, and the central laboratory of Xishuangbanna Tropical Botanical Garden,

630 Chinese Academy of Sciences. Thank Canopy Science Research Platform II for  
631 facility and data supporting.

632

### 633 **Reference**

634 Aparecido, L.M.T., Woo, S., Suazo, C., Hultine, K.R. and Blonder, B., 2020. High  
635 water use in desert plants exposed to extreme heat. *Ecol Lett*, 23(8): 1189-  
636 1200.

637 Bazzaz, F.A., 1979. The physiological ecology of plant succession. *Annual Review of*  
638 *Ecological Systematics*, 10: 351-371.

639 Blonder, B.W. et al., 2023. Plant water use theory should incorporate hypotheses  
640 about extreme environments, population ecology, and community ecology.  
641 *New Phytol*, 238: 2271-2283.

642 Blonder, B.W., Escobar, S., Kapas, R.E. and Michaletz, S.T., 2020. Low predictability  
643 of energy balance traits and leaf temperature metrics in desert, montane and  
644 alpine plant communities. *Funct Ecol*, 34(9): 1882-1897.

645 Blonder, B.W. and Michaletz, S.T., 2018. A model for leaf temperature decoupling  
646 from air temperature. *Agr Forest Meteorol*, 262: 354-360.

647 Bueno, A. et al., 2019. Effects of temperature on the cuticular transpiration barrier of  
648 two desert plants with water-spender and water-saver strategies. *J Exp Bot*,  
649 70(5): 1613-1625.

650 Burkner, P.C., 2017. brms: An R package for Bayesian multilevel models using stan. *J*  
651 *Stat Softw*, 80(1): 1-28.

652 Campbell, G.S. and Norman, J.M., 1998. *Introduction to environmental biophysics*.  
653 Springer, New York, xxi, 286 p. pp.

654 Chen, Y.J. et al., 2021. Hydraulic prediction of drought-induced plant dieback and  
655 top-kill depends on leaf habit and growth form. *Ecol Lett*, 24(11): 2350-2363.

656 Crawford, A.J., McLachlan, D.H., Hetherington, A.M. and Franklin, K.A., 2012. High  
657 temperature exposure increases plant cooling capacity. *Curr Biol*, 22(10):  
658 R396-R397.

659 Daudet, F.A., Silvestre, J., Ferreira, M.I., Valancogne, C. and Pradelle, F., 1998. Leaf  
660 boundary layer conductance in a vineyard in Portugal. *Agr Forest Meteorol*,  
661 89(3-4): 255-267.

662 Doughty, C.E. and Goulden, M.L., 2008. Are tropical forests near a high temperature  
663 threshold? *J Geophys Res-Bioge*, 113: G00B07.

664 Drake, J.E. et al., 2020. No evidence of homeostatic regulation of leaf temperature  
665 in *Eucalyptus parramattensis* trees: integration of CO<sub>2</sub> flux and oxygen isotope  
666 methodologies. *New Phytol*, 228(5): 1511-1523.

667 Drake, J.E. et al., 2018. Trees tolerate an extreme heatwave via sustained  
668 transpirational cooling and increased leaf thermal tolerance. *Global Change*  
669 *Biol*, 24(6): 2390-2402.

670 Fauset, S. et al., 2018. Differences in leaf thermoregulation and water use strategies  
671 between three co-occurring Atlantic forest tree species. *Plant Cell Environ*,  
672 41(7): 1618-1631.

673 Feng, X.L., Liu, R., Li, C.J., Zhang, H. and Slot, M., 2023. Contrasting responses of  
674 two C4 desert shrubs to drought but consistent decoupling of photosynthesis  
675 and stomatal conductance at high temperature. *Environ Exp Bot*, 209: 105295.

676 Fetcher, N., 1981. Leaf size and leaf temperature in tropical vines. *American*  
677 *Naturalist*, 117(6): 1011-1014.

678 Gates, D.M., 1968. Transpiration and leaf temperature. *Ann Rev Plant Physio*, 19:  
679 211-238.

680 Gates, D.M., 2003. *Biophysical ecology*. Dover Publications, Mineola, N.Y.

681 Gong, X.W., Leigh, A., Guo, J.J., Fang, L.D. and Hao, G.Y., 2023. Sand dune shrub  
682 species prioritize hydraulic integrity over transpirational cooling during an  
683 experimental heatwave. *Agr Forest Meteorol*, 336.

684 John-Bejai, C., Farrell, A.D., Cooper, F.M. and Oatham, M.P., 2013. Stress and  
685 survival in tropical environments contrasting physiological responses to excess  
686 heat and irradiance in two tropical savanna sedges. *Aob Plants*, 5: plt051.

687 Jones, H.G., 1999. Use of thermography for quantitative studies of spatial and  
688 temporal variation of stomatal conductance over leaf surfaces. *Plant Cell*  
689 *Environ*, 22(9): 1043-1055.

690 Jones, H.G., 2014. *Plants and microclimate - a quantitative approach to environmental*  
691 *plant physiology*. Cambridge University Press, University Printing House, UK.

692 Jones, H.G., Hutchinson, P.A., May, T., Jamali, H. and Deery, D.M., 2018. A practical  
693 method using a network of fixed infrared sensors for estimating crop canopy  
694 conductance and evaporation rate. *Biosyst Eng*, 165: 59-69.

695 Jones, H.G. and Rotenberg, E., 2011. *Energy, radiation and temperature regulation in*  
696 *plants*. eLS. John Wiley & Sons, Chichester.

697 Kitudom, N. et al., 2022. Thermal safety margins of plant leaves across biomes under  
698 a heatwave. *Sci Total Environ*, 806: 150416.

699 Knight, C.A. and Ackerly, D.D., 2002. An ecological and evolutionary analysis of  
700 photosynthetic thermotolerance using the temperature-dependent increase in  
701 fluorescence. *Oecologia*, 130(4): 505-514.

702 Körner, C., 2016. Plant adaptation to cold climates. *F1000Res*, 5: 2769.

703 Lambers, H., Chapin, F.S., III and Pons, T., 1998. Leaf energy budgets: effects of  
704 radiation and temperature, *Plant Physiological Ecology*. Springer New York,  
705 pp. 210-229.

706 Le Provost, G. et al., 2020. Land-use history impacts functional diversity across  
707 multiple trophic groups. *P Natl Acad Sci USA*, 117(3): 1573-1579.

708 Leigh, A. et al., 2012. Do thick leaves avoid thermal damage in critically low wind  
709 speeds? *New Phytol*, 194(2): 477-487.

710 Lin, H., Chen, Y.J., Zhang, H.L., Fu, P.L. and Fan, Z.X., 2017. Stronger cooling  
711 effects of transpiration and leaf physical traits of plants from a hot dry habitat  
712 than from a hot wet habitat. *Funct Ecol*, 31(12): 2202-2211.

713 Lüdecke, D., Ben-Shachar, M.S., Patil, I., Waggoner, P. and Makowski, D., 2021.

714 performance: An R package for assessment, comparison and testing of  
715 statistical models. *Journal of Open Source Software*, 16(60): 3139.

716 Mau, A.C., Reed, S.C., Wood, T.E. and Cavaleri, M.A., 2018. Temperate and tropical  
717 forest canopies are already functioning beyond their thermal thresholds for  
718 photosynthesis. *Forests*, 9(1): 47.

719 Michaletz, S.T. and Johnson, E.A., 2006. Foliage influences forced convection heat  
720 transfer in conifer branches and buds. *New Phytol*, 170(1): 197-197.

721 Michaletz, S.T. et al., 2015. Plant thermoregulation: Energetics, trait-environment  
722 interactions, and carbon economics. *Trends Ecol Evol*, 30(12): 714-724.

723 Miller, B.D., Carter, K.R., Reed, S.C., Wood, T.E. and Cavaleri, M.A., 2021. Only  
724 sun-lit leaves of the uppermost canopy exceed both air temperature and  
725 photosynthetic thermal optima in a wet tropical forest. *Agr Forest Meteorol*,  
726 301: 108347.

727 Mo, X.X., Shi, L.L., Zhang, Y.J., Zhu, H. and Slik, J.W.F., 2013. Change in  
728 phylogenetic community structure during succession of traditionally managed  
729 tropical rainforest in southwest china. *Plos One*, 8(7): e71464.

730 Monteiro, M.V., Blanusa, T., Verhoef, A., Hadley, P. and Cameron, R.W.F., 2016.  
731 Relative importance of transpiration rate and leaf morphological traits for the  
732 regulation of leaf temperature. *Aust J Bot*, 64(1): 32-44.

733 Monteith, J.L., 1973. Principles of environmental physics. Contemporary biology.  
734 American Elsevier Pub. Co., New York,, xiii, 241 pp.

735 Monteith, J.L. and Unsworth, M.H., 2013. Principles of environmental physics :  
736 plants, animals, and the atmosphere. Elsevier Academic Press, Amsterdam ;  
737 Boston.

738 Muir, C.D., 2019. tealeaves: an R package for modelling leaf temperature using  
739 energy budgets. *Aob Plants*, 11(6): plz054.

740 Muller, J.D., Rotenberg, E., Tatarinov, F., Oz, I. and Yakir, D., 2021. Evidence for  
741 efficient nonevaporative leaf-to-air heat dissipation in a pine forest under  
742 drought conditions. *New Phytol*, 232(6): 2254-2266.

743 Nobel, P.S., 2005. Physicochemical and environmental plant physiology. Elsevier  
744 Academic Press, Amsterdam, Boston.

745 Pau, S., Detto, M., Kim, Y. and Still, C.J., 2018. Tropical forest temperature  
746 thresholds for gross primary productivity. *Ecosphere*, 9(7): e02311.

747 Pérez-Harguindeguy, N. et al., 2013. New handbook for standardised measurement of  
748 plant functional traits worldwide. *Aust J Bot*, 61(3): 167-234.

749 Qiu, G.Y. et al., 2002. Comparison of the three-temperature model and conventional  
750 models for estimating transpiration. *Jarq-Japan Agricultural Research*  
751 *Quarterly*, 36(2): 73-82.

752 Rey-Sánchez, A.C., Slot, M., Posada, J.M. and Kitajima, K., 2017. Spatial and  
753 seasonal variation in leaf temperature within the canopy of a tropical forest.  
754 *Clim Res*, 71(1): 75-89.

755 Sadok, W., Lopez, J.R. and Smith, K.P., 2021. Transpiration increases under high-  
756 temperature stress: Potential mechanisms, trade-offs and prospects for crop  
757 resilience in a warming world. *Plant Cell Environ*, 44(7): 2102-2116.

758 Sánchez, J.M., Caselles, V., Niclos, R., Coll, C. and Kustas, W.P., 2009. Estimating  
759 energy balance fluxes above a boreal forest from radiometric temperature  
760 observations. *Agr Forest Meteorol*, 149(6-7): 1037-1049.

761 Schulze, E.D., Eller, B.M., Thomas, D.A., von Willert, D.J. and Brinckmann, E., 1980.  
762 Leaf Temperatures and Energy-Balance of *Welwitschia-Mirabilis* in Its  
763 Natural Habitat. *Oecologia*, 44(2): 258-262.

764 Slot, M., Garcia, M.N. and Winter, K., 2016. Temperature response of CO<sub>2</sub> exchange  
765 in three tropical tree species. *Funct Plant Biol*, 43(5): 468-478.

766 Slot, M. and Winter, K., 2017. In situ temperature response of photosynthesis of 42  
767 tree and liana species in the canopy of two Panamanian lowland tropical  
768 forests with contrasting rainfall regimes. *New Phytol*, 214(3): 1103-1117.

769 Smith, W.K., 1978. Temperatures of desert plants: another perspective on the  
770 adaptability of leaf size. *Science*, 201(4356): 614-616.

771 Smith, W.K. and Carter, G.A., 1988. Shoot Structural Effects on Needle Temperatures  
772 and Photosynthesis in Conifers. *Am J Bot*, 75(4): 496-500.

773 Steel, R.G.D., Torrie, J.H. and Dickey, D.A., 1997. Principles and procedures of  
774 statistics - a biometrical approach. *Biometrics*. McGraw-Hill, New York.

775 Still, C.J. et al., 2022. No evidence of canopy-scale leaf thermoregulation to cool  
776 leaves below air temperature across a range of forest ecosystems. *Proc Natl  
777 Acad Sci U S A*, 119(38): e2205682119.

778 Still, C.J. et al., 2021. Imaging canopy temperature: shedding (thermal) light on  
779 ecosystem processes. *New Phytol*, 230(5): 1746-1753.

780 Thorpe, M.R. and Butler, D.R., 1977. Heat transfer coefficients for leaves on orchard  
781 apple trees. *Boundary-Layer Meteorology*, 12: 61-73.

782 Tomlinson, K.W. et al., 2013. Leaf adaptations of evergreen and deciduous trees of  
783 semi-arid and humid savannas on three continents. *Journal of Ecology*, 101(2):  
784 430-440.

785 Urban, J., Ingwers, M.W., McGuire, M.A. and Teskey, R.O., 2017. Increase in leaf  
786 temperature opens stomata and decouples net photosynthesis from stomatal  
787 conductance in *Pinus taeda* and *Populus deltoides* x *nigra*. *J Exp Bot*, 68(7):  
788 1757-1767.

789 Vinod, N. et al., 2023. Thermal sensitivity across forest vertical profiles: patterns,  
790 mechanisms, and ecological implications. *New Phytol*, 237(1): 22-47.

791 Vogel, S., 2005. Living in a physical world V. Maintaining temperature. *J Biosciences*,  
792 30(5): 581-590.

793 Vogel, S., 2009. Leaves in the lowest and highest winds: temperature, force and shape.  
794 *New Phytol*, 183(1): 13-26.

795 Wallace, R.H. and Clum, H.H., 1938. Leaf temperatures. *Am J Bot*, 25(2): 83-97.

796 Zhang, J.L., 2007. Phenology, leaf structure and function, and seasonal variation in  
797 photosynthesis of woody plants in a dry-hot valley of Yuanjiang, southwestern  
798 China, Xishuangbanna Tropical Botanical Garden, Kunming, Yunnan.

799 Zhang, J.L., Poorter, L., Hao, G.Y. and Cao, K.F., 2012. Photosynthetic  
800 thermotolerance of woody savanna species in China is correlated with leaf life  
801 span. *Annals of Botany*, 110(5): 1027-1033.



802 Zhang, S.B., Wen, G.J. and Yang, D.X., 2019. Drought-induced mortality is related to  
803 hydraulic vulnerability segmentation of tree species in a savanna ecosystem.  
804 *Forests*, 10(8): 697.

805 Zhang, Y. et al., 2020. A proposed method for simultaneous measurement of cuticular  
806 transpiration from different leaf surfaces in *Camellia sinensis*. *Front Plant Sci*,  
807 11: 420.

808

809 Table 1 Site information (Kitudom et al., 2022)

Site	Abbreviation	Location	Elevation (m)	MAP (mm)	MAT (°C)	$Ta_{max}$ (°C)	$Ta_{min}$ (°C)	RH (%)	Canopy height (m)
Savanna woodland	SAV	23°28'N, 102°10'E	481	733	25.0	45.1	26.5	62 (53)	4-6
Tropical rain forest	TRF	21°22'N, 101°34'E	704	1415	22.7	38.6	18.6	80 (65)	>50
Subtropical broad-leaved forest	STF	24°32'N, 101°02'E	2501	1931	11.8	28.7	12.2	81 (60)	25-30
Temperate mixed forest	TEF	27°00'N, 100°13'E	3240	1300	8.7	26.8	9.1	65 (57)	25-30

810

811  $Ta_{max}$  and  $Ta_{min}$ , the maximum and minimum air temperature above the canopy during measurement, averaged by all the measure points on the  
 812 canopy; MAP, mean annual precipitation; MAT, mean annual temperature; RH, average relative humidity in 2019, the values in brackets are the  
 813 average RH during measurement.

814

815

816 Table 2 The investigated leaf traits (Kitudom et al., 2022).

Class	Leaf traits	Abbreviation (unit)
Morphological trait	Leaf Area	Area (cm <sup>2</sup> )
	Perimeter	P (cm)
	Leaf length	Length (cm)
	Leaf width	Width (cm)
	Length/Width	L/W
	The ratio of perimeter to area	P/A (cm <sup>-1</sup> )
	Angle	Angle (°)
Optical trait	Reflectivity	Ref (%)
	Absorptivity	Abs (%)
	Transmissivity	Trans (%)
	Greenness	Greenness
Material property	Leaf fresh mass density	Density.f (g cm <sup>-3</sup> )
	Leaf dry mass density	Density.d (g cm <sup>-3</sup> )
	Water content	WC (%)
	Leaf mass per area	LMA (g cm <sup>-2</sup> )
Anatomical trait	Leaf thickness	Thickness (μm)
	Thickness of upper epidermis	Epidermis_up (μm)
	Thickness of lower epidermis	Epidermis_low (μm)
	Thickness of spongy tissue	Spongy (μm)
	Thickness of palisade tissue	Palisade (μm)
	Leaf vein density	Vein density (mm <sup>-1</sup> )
	Stomata size	St.size (μm)
	Stomata density	St.density (No mm <sup>-2</sup> )
	Stomata size <sup>2</sup> × Stomata density	SPI (mm <sup>-1</sup> )
	Physiological trait	Maximum photosynthesis rate
Maximum transpiration rate		$Tr_{\max}$ (mmol m <sup>-2</sup> s <sup>-1</sup> )
Maximum stomatal conductance		$g_{\max}$ (mol m <sup>-2</sup> s <sup>-1</sup> )
Photosynthetic thermal tolerance		$T_{\text{crit}}$ (°C)

817

818

819 Table 3 Range of leaf temperature (Tl) and temperature difference between leaf and  
 820 air (dT).

Site	Tl range (°C)	dT range (°C)
	Mean ± SE	Mean ± SE
SAV	26.2 ± 0.11 ~ 46.0 ± 0.51	-1.3 ± 0.27 ~ 1.1 ± 0.43
TRF	18.2 ± 0.05 ~ 42.4 ± 0.91	-0.9 ± 0.11 ~ 2.5 ± 0.52
STF	11.1 ± 0.20 ~ 33.3 ± 0.66	-1.2 ± 0.11 ~ 2.9 ± 0.44
TEF	8.4 ± 0.11 ~ 33.3 ± 2.07	-0.8 ± 0.12 ~ 4.9 ± 1.44

821 SAV, savanna woodland; TRF, tropical rain forest; STF, subtropical evergreen broad-  
 822 leaved forest; TEF, temperate mixed forest.

823